Circulation Journal
Official Journal of the Japanese Circulation Society
http://www.j-circ.or.jp

ORIGINAL ARTICLE
Pulmonary Circulation

Role of Endothelial Nitric Oxide Synthase and Collagen Metabolism in Right Ventricular Remodeling due to Pulmonary Hypertension

Suvd Nergui, MD, PhD; Yoshihiro Fukumoto, MD, PhD; Zhulanqiqige Do.e, MD, PhD; Sota Nakajima, MD, PhD; Toru Shimizu, MD, PhD; Shohei Ikeda, MD; Md. Elias-Al-Mamun, PhD; Hiroaki Shimokawa, MD, PhD

Background: Pulmonary hypertension (PH) causes elevated right ventricular (RV) systolic pressure, RV remodeling and finally RV failure to death. However, the mechanisms of RV remodeling in PH remain to be fully elucidated.

Methods and Results: RV autopsy samples from 6 PH patients with RV failure against 3 age- and sex-matched controls were first examined. Next, RV remodeling in 2 mouse models of chronic hypoxia-induced PH with endothelial nitric oxide synthase-deficient ($eNOS^{-/-}$) and collagenase-resistant knock-in ($Col^{R/R}$) mice were examined. In humans, RV failure was associated with RV hypertrophy, interstitial and perivascular fibrosis, decreased RV capillary density and increased macrophage recruitment. Furthermore, immunostaining showed that perivascular matrix metalloproteinase-2 was increased in PH patients with RV failure. In animals, both hypoxic $eNOS^{-/-}$ and $Col^{R/R}$ mice developed a greater extent of RV hypertrophy, perivascular remodeling and macrophage infiltration compared with wild-type mice. Capillary rarefaction was developed in hypoxic $eNOS^{-/-}$ mice, while $Col^{R/R}$ mice were able to increase their capillary density in the RV in response to chronic hypoxia. Both mouse models showed increased autophagy even under normoxic condition.

Conclusions: These results indicate that RV remodeling occurs early during PH development through fibrosis, perivascular remodeling, capillary rarefaction and autophagy, in which the eNOS pathway and collagen metabolism might be involved. (*Circ J* 2014; **78:** 1465–1474)

Key Words: Endothelial nitric oxide synthase; Inflammatory cell; Pulmonary hypertension; Rho-kinase; Right ventricular fibrosis

Pulmonary hypertension (PH) is a fatal disease characterized by increased pulmonary vascular resistance, resulting in an impaired right ventricular (RV) function due to increased RV afterload and contractile abnormality of the RV.[1–3] The disease is progressive in nature, leading to RV hypertrophy (RVH) and ultimately RV failure and death within less than 5 years after diagnosis.[1,4] Mortality of PH patients is closely associated with alterations in RV hemodynamic variables, such as mean pulmonary artery pressure, mean right atrial pressure and cardiac index.[4] Despite the recent advances in medical therapy for PH, there is no cure for the disorder, and cellular and molecular mechanisms of RV remodeling and failure in PH still remain to be fully elucidated.[5]

RV is different from left ventricle (LV) embryologically, macroscopically, ultrastructurally, biochemically and hemodynamically.[6] Under normal conditions, smaller and crescent-shaped RV wall thickness is only one-fifth of that of the LV, and the RV has a higher proportion of the α-myosin heavy chain isoform that results in a more rapid but less energy efficient contraction.[7] Furthermore, coronary blood flow to the RV is roughly balanced between systolic and diastolic time periods, while a majority of the flow occurs in the diastole in the LV wall.[8] The RV has greater resistance to ischemia compare to the LV and has better adaptation to volume overload states, while LV has better adaptation to pressure overload states.[9] Thus, the increase in RV afterload might not be similar to that in the LV in response to pharmacological therapies.[10]

Nitric oxide (NO) synthesized by endothelial cells (eNOS) is an important downstream signaling molecule in the cardiovascular system.[11] The protective effects of NO on vascular

Received December 25, 2013; revised manuscript received March 4, 2014; accepted March 10, 2014; released online April 4, 2014 Time for primary review: 32 days
Department of Cardiovascular Medicine, Tohoku University Graduate School of Medicine, Sendai, Japan
The Guest Editor for this article was Masaaki Ito, MD.
Suvd Nergui won the First Place of the Young Investigator Award for International Students during the 2014 JCS Meeting, Tokyo.
Mailing address: Yoshihiro Fukumoto, MD, PhD, Department of Cardiovascular Medicine, Tohoku University Graduate School of Medicine, 1-1 Seiryo-machim, Aoba-ku, Sendai 980-8574, Japan. E-mail: fukumoto@cardio.med.tohoku.ac.jp
ISSN-1346-9843 doi:10.1253/circj.CJ-13-1586

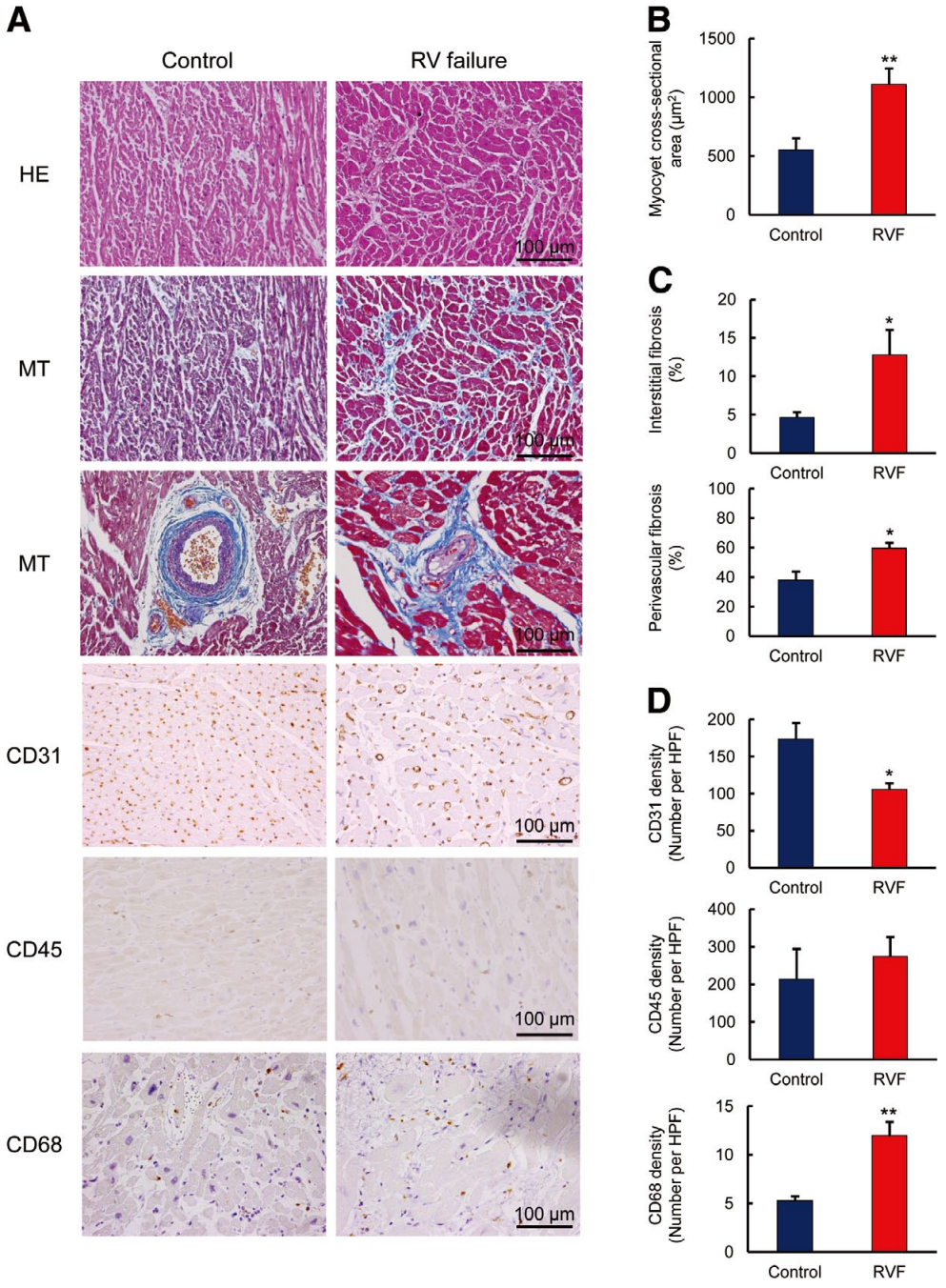

Figure 1. Histological findings of RV samples from PH patients. (**A**) Representative histological micrographs of the RV stained with hematoxylin-eosin (HE), Masson trichome (MT), CD31, CD45 and CD68 in a control (**Left**) and in a PH patient with RV failure (**Right**). (**B**–**D**) Quantitative analysis of a cardiomyocyte cross-sectional area (**B**), interstitial and perivascular fibrosis (**C**), and density of CD31-, CD45- and CD68-positive cells (**D**) in controls (n=3) and PH patients with RV failure (n=6). Results are expressed as mean±SEM. *P<0.05, **P<0.01 vs. control. RV, right ventricular; PH, pulmonary hypertension.

smooth muscle cells, such as relaxation and inhibition of proliferation and vascular remodeling, have been well documented previously.[12,13] Furthermore, the repair process of LV hypertrophy, fibrosis and angiogenesis caused by pressure overload are also dependent on NO production by eNOS.[14] The Rho/Rho-kinase pathway negatively regulates eNOS activity through the inhibition of cyclic GMP-dependent protein kinase Iα.[15,16] However, it is not known whether eNOS dysfunction and the Rho-kinase pathway are involved in the pathogenesis of RV remodeling in PH.

As cardiac interstitium and its fibrillar collagen matrix also play a critical role in determining cardiac performance,[17] the

disruption of collagen content and its balance with matrix metalloproteinases (MMPs) are involved in the hemodynamic changes, and consequently the integrity of collagen type I might have an influence on adverse RV remodeling.[18] Furthermore, pressure overload-induced LV remodeling is associated with impaired mitochondrial morphology and cardiac function, where autophagy has been implicated in inducing and maintaining inflammation of the heart.[19] It has been also reported that pathological LV hypertrophy is associated with impaired coronary angiogenesis.[20]

However, it remains to be examined whether those molecular and cellular mechanisms of LV remodeling are also involved in the pathogenesis of RV remodeling in PH. In the present study, we thus addressed this important issue, using human autopsy RV samples and 2 mouse models of hypoxia-induced PH with eNOS-deficient ($eNOS^{-/-}$) and collagenase-resistant ($Col^{R/R}$) mice.

Methods

In the human autopsy protocol, we confirmed the principles outlined in the Declaration of Helsinki, and the Ethical Committees of Tohoku University Hospital approved the study protocol. In the animal experiments, we confirmed the Guide for the Care and Use of Laboratory Animals (Institute of Laboratory Animal Resources, 1996), and all the procedures were performed according to the protocols approved by the Institutional Committee for the Use and Care of Laboratory Animals of Tohoku University.

Human Autopsy Samples

We examined 6 RV autopsy samples from PH patients with RV failure, who were aged from 27 to 72 years old; samples from 3 age- and sex-matched controls who died of non-cardiac causes were also examined (Table S1).

Animals

Male mice that were 7 weeks old were used. The $eNOS^{-/-}$ mice were originally provided by P. Huang (Harvard Medical School, Boston, MA, USA),[21] which were backcrossed to C57BL/6 mice over 10 generations. Thus, C57BL/6 mice were used as a wild-type (WT) control.[21] $Col^{R/R}$ mice and their WT controls were purchased from the Jackson Laboratory (Bar Harbor, MN, USA).[22] The interstitial collagenases of the MMP family initiate degradation of type I collagen by cleavage at a single highly conserved site between Gly^{775} and Ile^{776} of the $\alpha 1(1)$ chain.[23] The mice used in the present study were with a targeted mutation in both alleles of Col1a1 ($Col1a1^{tml\ Jae}$ or $Col^{R/R}$) that yields amino acid substitutions around the collagenase cleavage site in the $\alpha 1(1)$ chain, which render collagen that is completely resistant to attack by the collagenase MMP family (MMP-1/collagenase-1, MMP-8/collagenase-2 and MMP-13/collagenase-3).[24,25]

The animals were exposed to normoxia or hypoxia for 3 weeks. Hypoxic mice were housed in an acrylic chamber with a non-recirculating gas mixture of 10% O_2 and 90% N_2 produced by an adsorption-type oxygen concentrator to utilize exhaust air, while normoxic mice were provided with room air (21% O_2).[26] They were fed standard chow and water. The chamber was opened at least once every week for cleaning and feeding.

Hemodynamic Measurements

Hemodynamic measurements were performed as described in the Supplementary File 1.

Histological Analysis

Histological analyses were performed in autopsy samples of the RV from patients with PH and in mice at 10 weeks after the completion of a 3-week exposure to hypoxia and normoxia. Randomly selected 10 cardiomyocytes, 5 areas and 5 vessels for each human RV sample had their cardiomyocyte cross-sectional area analyzed and were also analyzed for interstitial and perivascular fibrosis after hematoxylin-eosin and Masson trichome staining, respectively, according to standard histological procedures. The cross-sectional area of cardiomyocytes was determined using microscopic images of samples with both a clear nucleus and intact cellular membrane in hematoxylin-eosin stained sections.[27]

The whole mice heart was fixed with 10% buffered formalin for 24–48 h and then embedded in paraffin wax, and cut into 3-μm-thick sections that were perpendicular to the long axis of the RV. The sections were then stained with hematoxylin-eosin and Masson trichrome according to standard histological procedures. For each animal, the wall thickness of the RV was measured at 20 points and the average was calculated. A computer-aided manipulator program (KS-Analyzer v 2.10; Keyence Corp, Osaka, Japan) was used for the analysis. Up to 10 cardiomyocytes were analyzed per heart for cross-sectional area. The area of myocardial interstitial fibrosis was determined using Masson trichome-stained sections of the RV and was expressed as the percent of interstitial fibrosis, as described previously.[28] On average, 10 areas were analyzed per heart.

To evaluate the perivascular fibrosis, short-axis images of coronary arteries were scanned at ×40 magnification. The area of perivascular fibrosis was calculated as the ratio of the fibrosis area surrounding the vessel to the total vessel area. On average, 7 vessels were analyzed per heart, and the perivascular nucleus was calculated, as previously described.[29]

Immunohistochemistry

The human RV autopsy samples were immunostained for antibodies, including CD31 (M0823, Dako, 1:40), CD45 (M0701, Dako, 1:50), CD68 (M0876, Dako, 1:100), and MMP2 (NCL-MMP2-507, Novocastra, 1:40). Immune complexes were detected by using biotinylated secondary antibodies, horseradish-peroxidase-conjugated streptavidin, and the peroxidase substrate, diaminobenzidine. After staining with hematoxylin, mounting solution and cover slips were added to the sections. Slides were observed with a light microscope. Ten random areas were analyzed for CD31 and CD68. Due to the low density of CD45, continuous 200 high power field (HPF) were analyzed. Five random vessels were analyzed for perivascular MMP2. All the histological and immunohistological images were obtained using an Olympus DP70 (Olympus, Tokyo, Japan) and quantified with Adobe® Photoshop® CS3 Extended software (Adobe Systems).

Statistical Analysis

All results are expressed as mean±SEM. We assessed the differences in measured parameters in 2 groups using the unpaired t-tests for statistical analysis. A value of $P<0.05$ was considered to be statistically significant.

Results

Enhanced Myocardial Fibrosis and Inflammatory Cell Infiltration, and Reduced Angiogenesis in the RV of PH Patients

The PH patients who died of RV failure had severe RVH compared with the controls (cardiomyocyte cross-sectional area,

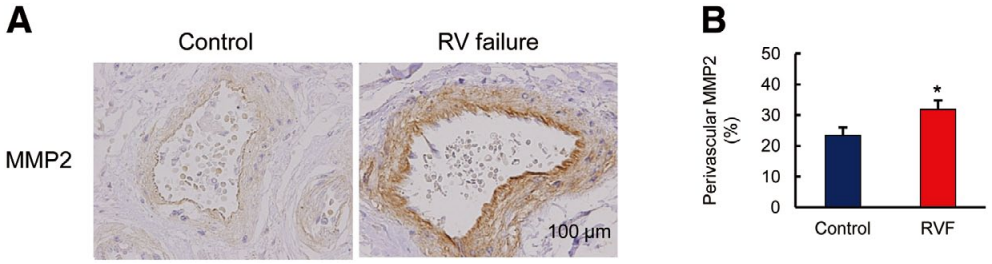

Figure 2. Immunostainings of RV samples from PH patients. (**A**) Representative histological micrographs of the RV stained with MMP2. (**B**) Quantitative analysis of perivascular MMP2 in controls (n=3) and PH patients with RV failure (n=6). Results are expressed as mean±SEM. *P<0.05, **P<0.01 vs. control. RV, right ventricular; PH, pulmonary hypertension; MMP2, matrix metalloproteinase.

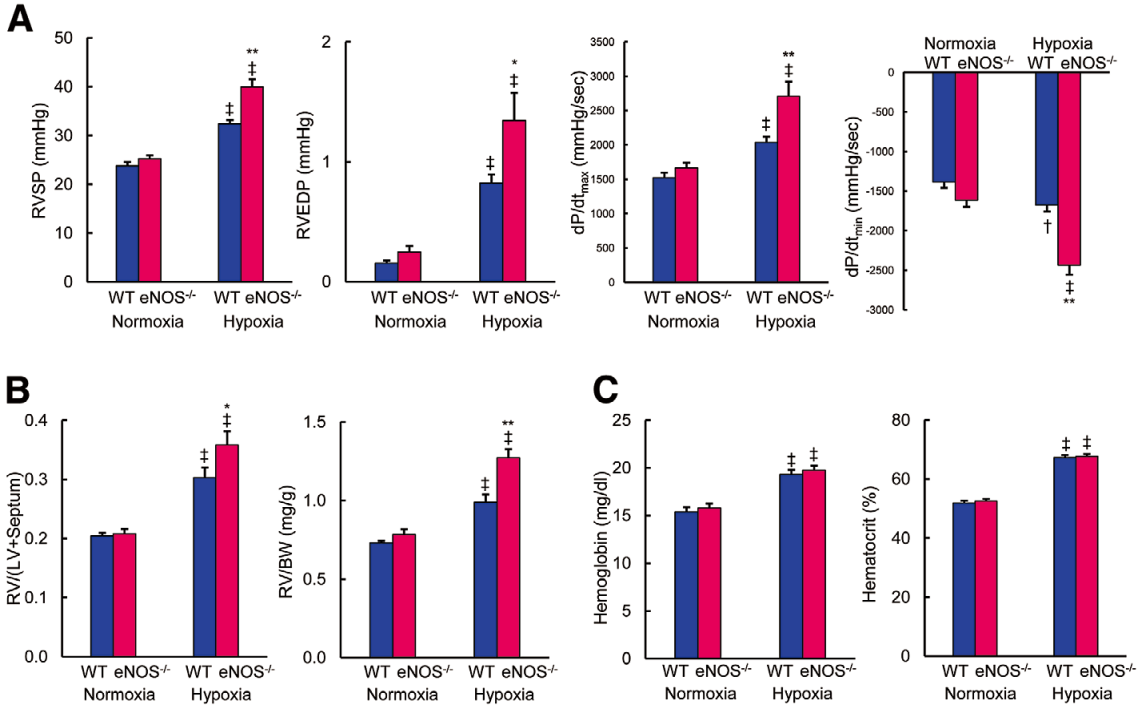

Figure 3. Hypoxia-induced RVH is enhanced in eNOS$^{-/-}$ mice. (**A**) RVSP and other hemodynamics were increased in response to chronic hypoxia in eNOS$^{-/-}$ mice compared with WT mice (n=10–13). (**B**) The extent of RVH is shown as the ratio of the RV to LV+septum and that of RV to body weight (n=7–10). (**C**) Hematocrit and hemoglobin (n=11–13). Results are expressed as mean±SEM. *P<0.05, **P<0.01 vs. hypoxic WT mice, †P<0.05, ‡P<0.01 vs. normoxic control. RVH, right ventricular hypertrophy; eNOS$^{-/-}$, endothelial nitric oxide synthase-deficient mice; RVSP, right ventricular systolic pressure; WT, wild-type.

1,107±139 vs. 547±105 μm^2, P<0.01; Figures 1A,B) along with enhanced increased interstitial and perivascular fibrosis (12.8±3.3 vs. 4.6±0.7% and 62.4±3.3 vs. 37.6±6.2%, respectively, both P<0.05; Figures 1A,C).

RV failure was associated with reduced capillary density, detected as a CD31-positive cell (number per HPF, 105±9 vs. 173±23, P<0.05; Figures 1A,D) and a tendency for an increased number of CD45-positive cells in the RV (272±54 vs. 213±81 per 20 continues HPF; Figures 1A,D). Interestingly, the number of CD68-positive cells in the RV free wall was significantly higher in the PH patients compared with the controls (11.9±1.5 vs. 5.2±0.6 per HPF, P<0.01; Figures 1A,D).

Enhanced Perivascular MMP2 Expression in the RV of PH Patients

The immunoreactivity of perivascular MMP2 was significantly increased in the PH patients compared with the controls (31.9±3.0 vs. 23.3±2.8%, P<0.05; Figures 2A,B).

Enhanced RVH in Hypoxic eNOS$^{-/-}$ Mice

Next, the role of eNOS in the pathogenesis of RV dysfunction using eNOS$^{-/-}$ mice with chronic exposure to hypoxia was examined. Under normoxic conditions, RV hemodynamic measurements and RVH were comparable between WT and eNOS$^{-/-}$ mice. However, after a 3-week exposure to hypoxia,

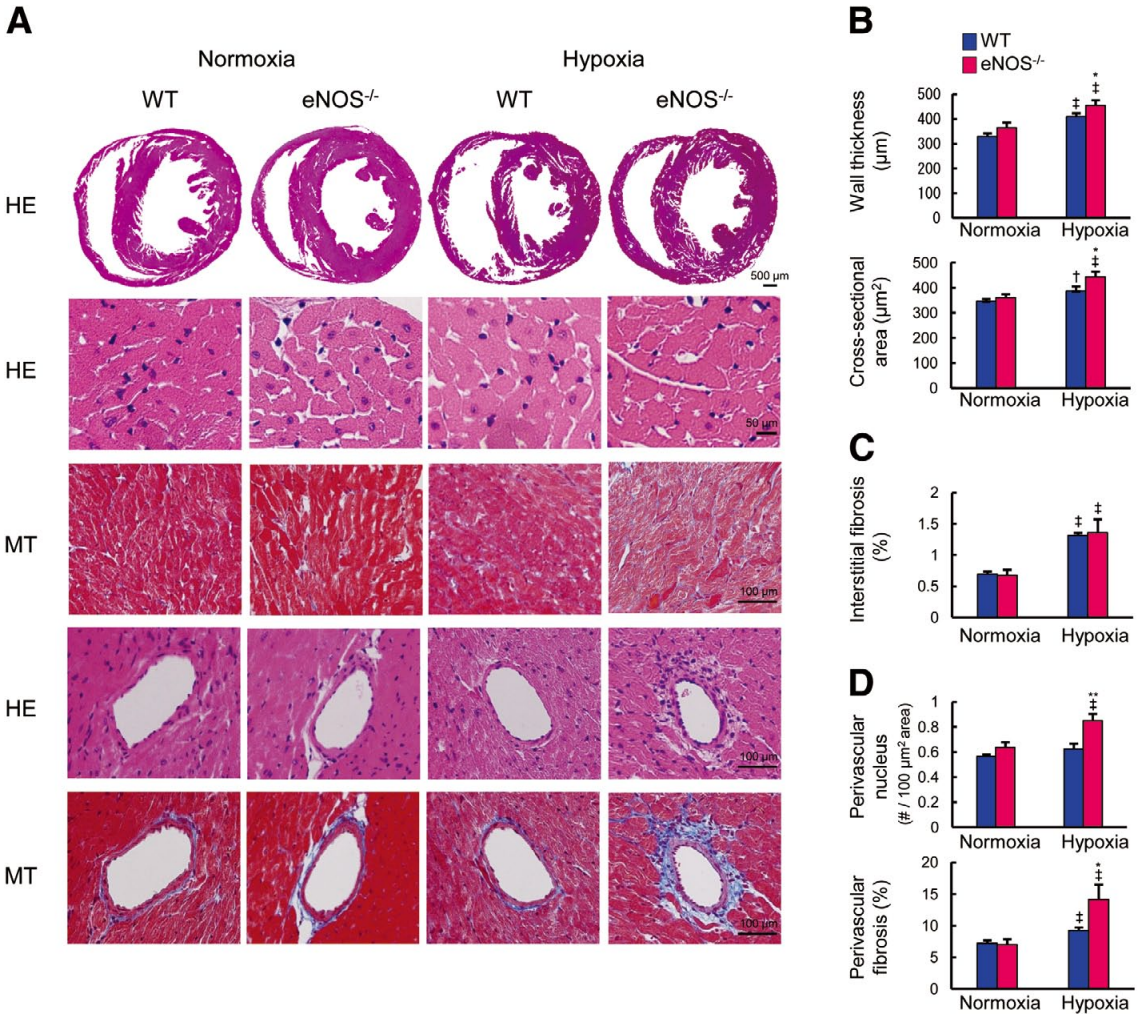

Figure 4. Hypoxia-induced RV remodeling is enhanced in eNOS$^{-/-}$ mice. (**A**) Representative histological micrographs of the RV stained with hematoxylin-eosin (HE) and Masson trichome (MT). (**B**–**C**) Quantitative analyses showed that the extent of hypoxia-induced RV remodeling was enhanced in eNOS$^{-/-}$ mice compared with WT mice, including RV free wall thickness (n=9–13) and cardiomyocyte cross-sectional area (n=7–12) (**B**), interstitial fibrosis (n=11–12) (**C**), and perivascular nucleus and fibrosis (n=7–12) (**D**). Results are expressed as mean±SEM. *P<0.05, **P<0.01 vs. hypoxic WT mice, †P<0.05, ‡P<0.01 vs. normoxic control. RV, right ventricular; eNOS$^{-/-}$, endothelial nitric oxide synthase-deficient mice; WT, wild-type.

RV systolic pressure (RVSP) and RV end-diastolic pressure (RVEDP) were significantly elevated in eNOS$^{-/-}$ mice as compared with WT mice (40.0±1.6 vs. 32.4±0.8 mmHg, P<0.01; 1.3±0.2 vs. 0.8±0.1 mmHg, P<0.05, respectively; **Figure 3A**), while systemic blood pressure in eNOS$^{-/-}$ mice was unchanged under hypoxia (normoxia vs. hypoxia; systolic blood pressure, 118±9 vs. 111±11 mmHg; diastolic blood pressure, 84±8 vs. 89±6 mmHg). Both RV dP/dt_{max} and RV dP/dt_{min} were significantly increased in hypoxic eNOS$^{-/-}$ mice compared with hypoxic WT mice (2,706±218 vs. 2,038±82 mmHg/s, –2,435±87 vs. –1,675±81 mmHg/s, both P<0.01; **Figure 3A**).

RV hypertrophy was more accelerated in hypoxic eNOS$^{-/-}$ mice as compared with hypoxic WT mice, as examined by the ratio of RV to LV+septum (0.36±0.02 vs. 0.30±0.02, P<0.05) and by the ratio of RV to bodyweight (1.27±0.06 vs. 0.99±0.05, P<0.01; **Figure 3B**). The ratio of lung weight to bodyweight, a potent parameter of pulmonary arteriopathy, was also significantly increased in hypoxic eNOS$^{-/-}$ mice compared with hypoxic WT mice (**Table S2**). In contrast, hemoglobin and hematocrit were equally elevated in hypoxic WT and eNOS$^{-/-}$ mice as compared with their normoxic counterparts (**Figure 3C**).

Enhanced RV Perivascular Remodeling in Hypoxic eNOS$^{-/-}$ Mice

RV wall thickness was significantly increased in response to hypoxia in WT mice, which was further accelerated in eNOS$^{-/-}$ mice (455±21 vs. 409±15 μm, P<0.05; **Figures 4A,B**). Similarly, a cross-sectional area of cardiomyocytes was significantly elevated in hypoxic eNOS$^{-/-}$ compared with hypoxic WT mice (444±20 vs. 386±20 μm^2, P<0.05; **Figures 4A,B**). Three weeks after hypoxia, RV interstitial fibrosis was equally increased in both genotypes (1.4±0.2 vs. 1.3±0.04%; **Figures 4A,C**). Interestingly, the number of perivascular nucleus and the extent of perivascular fibrosis in response to hypoxia were significantly

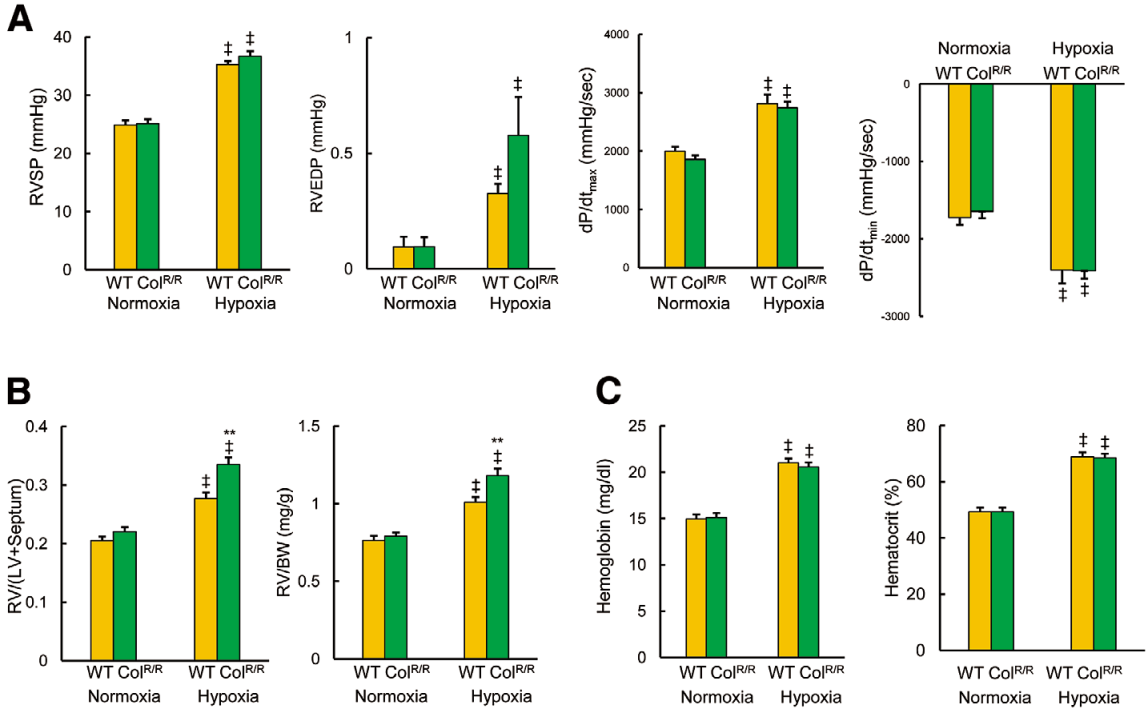

Figure 5. Hypoxia-induced RVH is enhanced in Col$^{R/R}$ mice. (**A**) RVSP and other hemodynamics were increased in response to chronic hypoxia (n=8–11). (**B**) RVH is shown as the ratio of RV to LV+Septum and that of RV to bodyweight (n=12–14). (**C**) Hematocrit and hemoglobin (n=14–17). Results are expressed as mean±SEM. **P<0.01 vs. hypoxic WT mice, ‡P<0.01 vs. normoxic control. RV, right ventricular; RVH, right ventricular hypertrophy; Col$^{R/R}$, collagenase-resistant knock-in mice; RVSP, right ventricular systolic pressure; LV, left ventricle.

accelerated in eNOS$^{-/-}$ compared with WT mice (0.85±0.05 vs. 0.63±0.04 per 100 μm^2 vessel area, P<0.01; 14.2±2.3 vs. 9.2±0.5%, P<0.05, respectively; **Figures 4A**,**D**).

Impaired Angiogenesis in Hypoxic eNOS$^{-/-}$ Mice

Although hypoxia significantly increased capillary density and the ratio of capillaries to cardiomyocytes in both genotypes, the extent was significantly lower in eNOS$^{-/-}$ compared with WT mice (840±20 vs. 925±32 capillaries to 1 mm^2, P<0.05; 0.90±0.04 vs. 1.05±0.05 capillaries to cardiomyocytes, P<0.05; **Figures S1A**,**B**). Furthermore, the number of F4/80-positive macrophages in the RV was greater in eNOS$^{-/-}$ compared with WT mice (6.9±1.5 vs. 3.9±0.9 cells per RV free wall, P<0.05; **Figures S1A**,**C**).

Enhanced RVH in Hypoxic Col$^{R/R}$ Mice

To further examine the role of collagen metabolism in the RV wall, chronic hypoxia-induced RV remodeling in WT and Col$^{R/R}$ mice was examined. Under normoxic conditions, hemodynamic variables were comparable between the 2 genotypes. In response to chronic hypoxia, RVSP was equally increased in Col$^{R/R}$ and WT mice (37±1 vs. 35±1 mmHg; **Figure 5A**). This was also the case for RVEDP (0.6±0.2 vs. 0.3±0.04 mmHg), dP/dt$_{max}$ (2,742±108 vs. 2,812±159 mmHg/s) and RV dP/dt$_{min}$ (–2,414±100 vs. –2,401±130 mmHg/s; **Figure 5A**). In contrast, systemic blood pressure in Col$^{R/R}$ mice was unchanged under hypoxia (normoxia vs. hypoxia; systolic blood pressure, 114±2 vs. 115±2 mmHg; diastolic blood pressure, 77±3 vs. 80±2 mmHg).

Interestingly, chronic hypoxia caused a greater extent of RVH in Col$^{R/R}$ compared with WT mice (0.33±0.01 vs. 0.28±0.01, P<0.01; **Figure 5B**). This was also the case for the ratio of RV to bodyweight (1.18±0.05 vs. 1.01±0.03, P<0.01; **Figure 5B**). In contrast, the ratio of lung weight to bodyweight was comparable between the 2 genotypes (**Table S3**). Hemoglobin and hematocrit levels were equally increased in response to hypoxia in WT and Col$^{R/R}$ mice (**Figure 5C**).

RV wall thickness was significantly increased in response to hypoxia in Col$^{R/R}$ mice compared with WT mice (450±24 vs. 397±14 μm, P<0.05; **Figures 6A**,**B**). Furthermore, a cross-sectional area of cardiomyocytes was significantly increased in response to hypoxia to a greater extent in Col$^{R/R}$ compared with WT mice (343±15 vs. 297±14 μm^2, P<0.05; **Figures 6A**,**B**).

No Enhancement of RV Vascular Remodeling in Hypoxic Col$^{R/R}$ Mice

Hypoxia caused a comparable extent of increased interstitial fibrosis in WT and Col$^{R/R}$ mice (0.63±0.04 vs. 0.62±0.05%; **Figures 6A**,**C**). To examine collagen accumulation due to the resistance of degradation in hypoxia in Col$^{R/R}$ mice, which could occur around blood vessels, vascular remodeling such as the number of nucleus and the area of fibrosis around the vessel of RV free wall was examined. Hypoxia also caused a comparable extent of vascular remodeling in WT and Col$^{R/R}$ mice, as evaluated by the number of nucleus (8.2±0.5 vs. 7.7±0.8 nucleus/100 μm^2 vessel area) and by perivascular fibrosis (8.58±0.96 vs. 8.10±0.94%; **Figures 6A**,**D**). In contrast, capillary density was significantly increased in hypoxic Col$^{R/R}$ mice compared

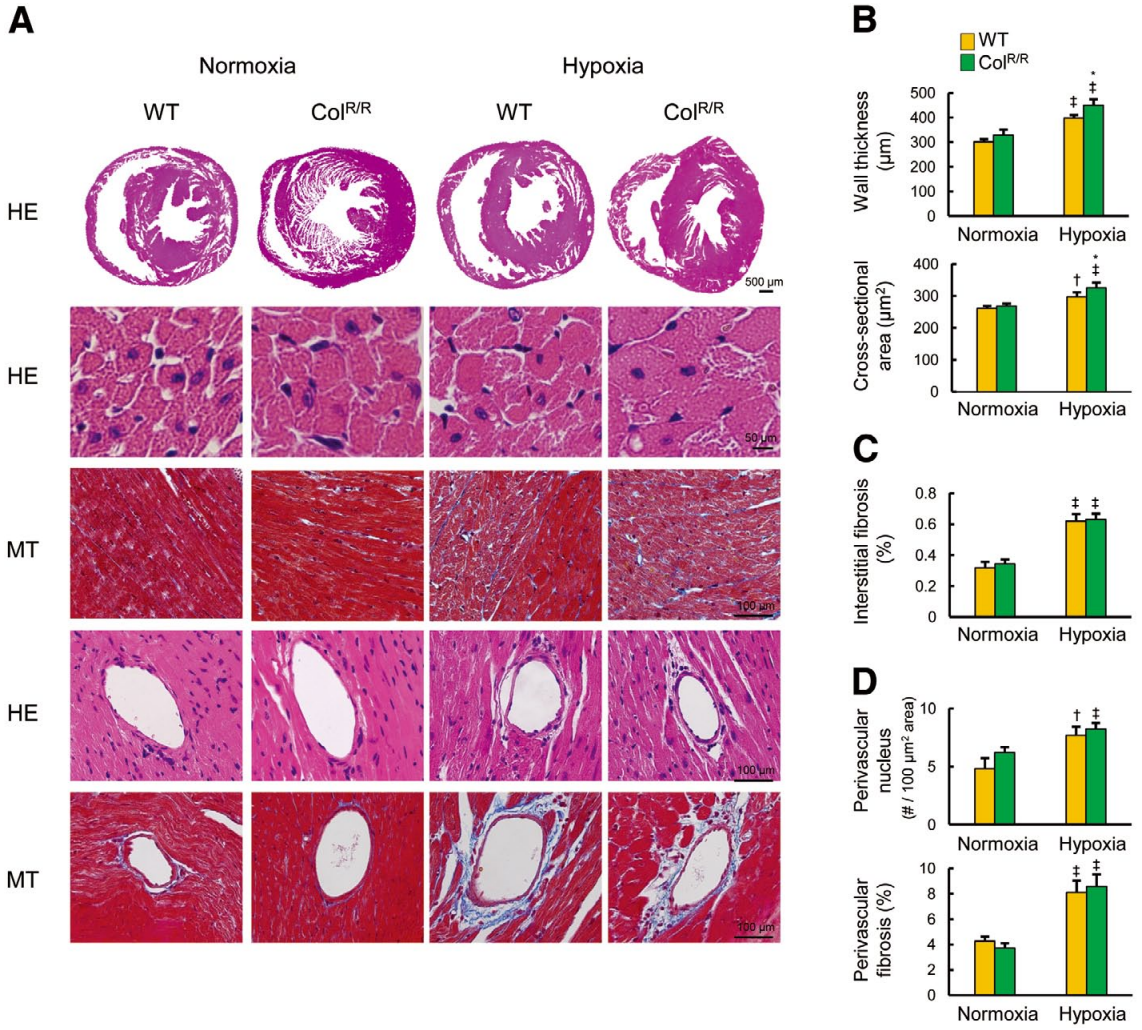

Figure 6. Hypoxia-induced RV remodeling is enhanced in Col$^{R/R}$ mice. (**A**) Representative histological micrographs of the RV stained with hematoxylin-eosin (HE) or Masson trichome (MT). (**B**) RV free wall thickness (n=10–12) and cardiomyocyte cross-sectional area (n=9–13). (**C**) Interstitial fibrosis (n=9–13). (**D**) Perivascular nucleus and fibrosis (n=10–12). Results are expressed as mean±SEM. *P<0.05 vs. hypoxic WT mice, †P<0.05, ‡P<0.01 vs. normoxic control. RV, right ventricular; Col$^{R/R}$, collagenase-resistant knock-in mice.

with WT mice (475±14 vs. 399±16.7 capillaries to 1 mm^2, P<0.01; 1.00± 0.05 vs. 0.85±0.03 capillaries to cardiomyocytes, P<0.05; Figures S2A,B).

Rho-Kinase Activity in eNOS$^{-/-}$ and Col$^{R/R}$ Mice

The immunoreactivity of p-MBS, a marker of Rho-kinase activity, was significantly increased in both hypoxic eNOS$^{-/-}$ and Col$^{R/R}$ mice compared to the hypoxic WT mice, whereas there was no difference noted among normoxic and hypoxic groups of eNOS$^{-/-}$ and Col$^{R/R}$ mice for ROCK1 immunoreactivity (3.0±0.3 vs. 1.82±0.1%, P<0.01; 3.4±0.6 vs. 2.1±0.1%, P<0.05; Figures S3A,4B). Interestingly, we found that there was an increased ROCK2 immunoreactivity in the hypoxic eNOS$^{-/-}$ mouse group compared to the hypoxic WT group (4.2±0.2 vs. 3.4±0.3, P<0.05; Figure S3B). However, we did not observe a significant difference for ROCK2 between the normoxic and hypoxic groups of Col$^{R/R}$ mice (Figure S4B).

Autophagy in eNOS$^{-/-}$ and Col$^{R/R}$ Mice

Increased mitochondrial damage might enhance autophagy, as evaluated by the number of autophagosomes/autolysosomes found using electron microscopy.[30] Interestingly, even under normoxic conditions, the number of autophagosomes/autolysosomes was significantly increased in eNOS$^{-/-}$ compared with WT mice (15.0±1.8 vs. 9.0±0.4 per HPF, P<0.05; Figures S5A–C), whereas hypoxia increased the number of autophagosomes in the RV wall in WT mice but not in eNOS$^{-/-}$ mice (Figures S5A–C).

The number of autophagosomes was significantly greater in Col$^{R/R}$ mice compared with WT mice under normoxic conditions (7.3±0.5 vs. 4.2±1.1 per HPF, P<0.05), and this was also the case for hypoxia (8.7±0.8 vs. 4.7±1.6 per HPF, P<0.05; Figure S5D).

Discussion

Although the molecular mechanisms of RV remodeling remain to be elucidated,[4,31] RV dysfunction could be caused by multiple cellular mechanisms, including oxidative stress, inflammation, fibrosis, apoptosis and metabolic remodeling.[32] The present study demonstrates that RV remodeling occurs early during the course of PH, as shown by human autopsy samples and experimental models.

The novel findings of the present study are as follows: (1) RV remodeling through increased interstitial and perivascular fibrosis and inflammatory cell recruitments; (2) capillary rarefaction, vascular remodeling, and perivascular MMP2 might play essential roles in the development of RV failure; (3) eNOS exerts crucial inhibitory effects on perivascular remodeling, increased inflammatory cells, capillary rarefaction and autophagosomes; and (4) collagen metabolism might contribute to the development of RVH and autophagosomes. To the best of our knowledge, this is the first report that demonstrates the role of eNOS and collagen metabolism in the pathogenesis of RV remodeling in PH.

RV Remodeling in PH

The present study results, which used the autopsy RV samples from patients with PH, showed the development of severe cardiomyocyte hypertrophy and interstitial/perivascular fibrosis as compared with the controls. As the presence of endothelial dysfunction has been already reported,[33,34] reduced availability of NO might be partially involved in these changes, as eNOS$^{-/-}$ mice showed enhanced RV cardiomyocyte hypertrophy and interstitial/perivascular fibrosis in response to chronic hypoxia. Col$^{R/R}$ mice also had increased RVSP and RVH in response to chronic hypoxia, although their RV hemodynamics was comparable with those in hypoxic WT mice. Col$^{R/R}$ mice also showed enhanced cardiomyocyte hypertrophy but not interstitial/perivascular fibrosis compared with hypoxic WT mice, suggesting some different roles of NO deficiency and collagenase resistance in the pathogenesis of the fibrosis.

RV Remodeling and MMPs in PH

As hypertension progresses with increased fibrosis, MMPs are involved in the breakdown of extracellular matrix, specifically type I collagen.[35] Thus, immunostainings for MMP2 in RV autopsy samples were carried out, as they are frequently involved in cardiovascular diseases.[36] Interestingly, perivascular MMP2 was significantly elevated in RV failure patients. Furthermore, higher immunoreactivity of MMP2 was noted around the coronary artery, suggesting its role in the vascular remodeling in PH. However, in the present study, we were unable to examine the issue regarding the specific inhibition for MMPs, which should be clarified in future studies.

Capillary Rarefaction in PH

The role of capillary rarefaction has not been systematically studied as a cause of RV failure in PH despite the fact that reduced capillary density and VEGF expression are known to play causative roles in pressure overload-induced LV failure.[20,37–39] It has been previously reported that RV failure patients without coronary artery disease can develop myocardial ischemia due to reduced capillary density.[39–41] Because eNOS has been implicated in angiogenesis in the LV through the phosphatidylinositol-3 kinase-Akt pathway,[42] the impairment of the pathway might also be involved in RV capillary rarefaction in PH.

In the present study, the RV failure autopsy samples showed severe capillary rarefaction compared with the controls. Because NO plays an important role in angiogenesis,[42] it was examined whether chronic hypoxia in eNOS$^{-/-}$ mice could cause capillary rarefaction. Indeed, hypoxic eNOS$^{-/-}$ mice had reduced capillary rarefaction compared with hypoxic WT mice, which was further confirmed by the ratio of capillaries to cardiomyocytes. Interestingly, chronic hypoxia did not compromise capillary density in Col$^{R/R}$ mice, suggesting that NO deficiency is more critical for capillary rarefaction compared with collagenase resistance, although MMPs are also important in angiogenesis.[43]

Inflammation and RV Failure in PH

The role of macrophage recruitment in the pathogenesis of RV failure in PH remains to be elucidated.[32] In the present study, both human RV samples from PH patients and hypoxic eNOS$^{-/-}$ mice showed an increased macrophage infiltration into the RV, whereas hypoxia was not sufficient enough to induce macrophage infiltration into the RV in Col$^{R/R}$ mice. Thus, further studies are needed to explore the types of macrophages and their specific roles in the development of RVH and RV failure development. Furthermore, in the present study, perivascular nucleus and fibrosis were calculated as indices of perivascular remodeling. We consider that some of them were F4/80-positive macrophages; however, other cell types were not characterized. This issue also remains to be clarified in future studies.

Rho-Kinase Activation in PH Patients With RV Failure

It was previously demonstrated that Rho-kinase activity is increased in the pulmonary arteries and circulating leukocytes of PH patients.[44] In the present study, it was found that Rho-kinase activity was increased in the RV of the PH model. These results suggest that the activated Rho-kinase pathway also plays an important role in the development of RV failure in PH. Indeed, it was recently demonstrated that the development of pressure overload-induced RV dysfunction can be suppressed in mice overexpressing dominant-negative Rho-kinase in cardiomyocytes.[45] An important downstream mediator of Rho is ROCK, which can regulate eNOS mRNA stability as well as the phosphorylation of eNOS; therefore, reduction of eNOS might be related to increased upstream, as shown by the p-MBS activity.[46,47]

Autophagy and RV Remodeling in PH

It has been previously reported that autophagy is enhanced in RV remodeling, which is caused by pulmonary arterial constriction in mice.[48] The present study demonstrated that autophagy is enhanced in both normoxic eNOS$^{-/-}$ and Col$^{R/R}$ mice compared with normoxic WT mice. Mitochondrial DNA plays an important role in inducing and maintaining inflammation in the heart,[19] and during PH development, it was reported that systemic activation of inflammation occurs,[49–51] which might be related to autophagy changes in the RV. Because increased autophagy was observed in normoxic eNOS$^{-/-}$ mice, it is possible that cardiomyocyte damage reached the maximum level under normoxia and could not be further increased in response to hypoxia, or that mildly increased RVSP was not able to induce autophagy. It might also be the reason for the spontaneous development of PAH in eNOS$^{-/-}$ mice. This point remains to be examined in future studies.

Study Limitations

Several limitations should be mentioned for the present study. First, the hypoxia-induced PH model in the present study does not fully recapitulate PH in humans (eg, absence of plexiform

lesions of the pulmonary artery in the present model). It might represent an initial compensated stage of RV remodeling in PH. Second, cardiac output was not examined by echocardiography because of technical limitations. Third, rescue experiments with $eNOS^{-/-}$ and $Col^{R/R}$ mice were not performed in order to further confirm the involvement of NO deficiency and collagenase resistance in the pathogenesis of RV remodeling in PH. Fourth, in the present study, we were unable to examine the possible unbalance between angiogenic and anti-angiogenic factors, which should be clarified in the next study. Fifth, the present study was performed in a hypoxia-induced PH model in mice; however, RV remodeling in PH should also be addressed in other models, such as a pulmonary artery banding model, in future studies. Finally, the extent of PH in the hypoxia-induced PH model in mice is mild as compared with that of rat PH models.[52] A suitable PH model in mice should be developed in the near future.

Clinical Implications

The present study has important clinical implications for the eNOS pathway and collagen metabolism in early RV remodeling in mildly increased RVSP. Currently, there is not any therapeutic intervention targeting RV dysfunction in PH patients. It remains to be examined in future studies what drug interventions can be used for PH and LV dysfunction that could improve those changes in RV remodeling. As RV dysfunction is a main cause of death in PH patients, it is essential to develop therapeutic strategies for not only pulmonary hemodynamics but also for RV function to improve the long-term survival of patients.

Conclusions

The present study demonstrates that RV remodeling begins early during the development process of PH through fibrosis, perivascular remodeling, capillary rarefaction and autophagy, for all of which the eNOS pathway and collagen metabolism might be involved.

Acknowledgments

The authors wish to thank A. Saito, C. Miyamoto, T. Hiroi, and Y. Watanabe for their excellent technical assistance.

This work was supported, in part, by the Grant-in-Aid for Scientific Research on Innovative Areas, the Grant-in-Aid for Tohoku University Global COE for Conquest of Signal Transduction Diseases with Network Medicine, and the Grants-in-Aid for Scientific Research, all of which are from the Ministry of Education, Culture, Sports, Science and Technology, Tokyo, Japan.

Disclosures

None.

References

1. Gaine SP, Rubin LJ. Primary pulmonary hypertension. *Lancet* 1998; **352:** 719–725.
2. Voelkel NF, Quaife RA, Leinwand LA, Barst RJ, McGoon MD, Meldrum DR, et al. Right ventricular function and failure: Report of a national heart, lung, and blood institute working group on cellular and molecular mechanisms of right heart failure. *Circulation* 2006; **114:** 1883–1891.
3. Fukumoto Y, Shimokawa H. Recent progress in the management of pulmonary hypertension. *Circ J* 2011; **75:** 1801–1810.
4. Humbert M, Sitbon O, Simonneau G. Treatment of pulmonary arterial hypertension. *N Engl J Med* 2004; **351:** 1425–1436.
5. D'Alonzo GE, Barst RJ, Ayres SM, Bergofsky EH, Brundage BH, Detre KM, et al. Survival in patients with primary pulmonary hypertension: Results from a national prospective registry. *Ann Intern Med* 1991; **115:** 343–349.
6. Greyson CR. Pathophysiology of right ventricular failure. *Crit Care Med* 2008; **36:** S57–S65.
7. Reiser PJ, Portman MA, Ning XH, Schomisch Moravec C. Human cardiac myosin heavy chain isoforms in fetal and failing adult atria and ventricles. *Am J Physiol* 2001; **280:** H1814–H1820.
8. Lowensohn HS, Khouri EM, Gregg DE, Pyle RL, Patterson RE. Phasic right coronary artery blood flow in conscious dogs with normal and elevated right ventricular pressures. *Circ Res* 1976; **39:** 760–766.
9. Dell'Italia LJ. The right ventricle: Anatomy, physiology, and clinical importance. *Curr Probl Cardiol* 1991; **16:** 653–720.
10. Johnson JA, West J, Maynard KB, Hemnes AR. ACE2 improves right ventricular function in a pressure overload model. *PloS One* 2011; **6:** e20828, doi:10.1371/journal.pone.0020828.
11. Huang PL. Mouse models of nitric oxide synthase deficiency. *J Am Soc Nephrol* 2000; **11**(Suppl 16)**:** S120–S123.
12. Shimokawa H, Tsutsui M. Nitric oxide synthases in the pathogenesis of cardiovascular disease: Lessons from genetically modified mice. *Eur J Physiol* 2010; **459:** 959–967.
13. Snyder SH, Jaffrey SR. Vessels vivified by Akt acting on NO synthase. *Nat Cell Biol* 1999; **1:** E95–E96, doi:10.1038/12093.
14. Kazakov A, Muller P, Jagoda P, Semenov A, Bohm M, Laufs U. Endothelial nitric oxide synthase of the bone marrow regulates myocardial hypertrophy, fibrosis, and angiogenesis. *Cardiovasc Res* 2012; **93:** 397–405.
15. Ming XF, Viswambharan H, Barandier C, Ruffieux J, Kaibuchi K, Rusconi S, et al. Rho GTPase/Rho kinase negatively regulates endothelial nitric oxide synthase phosphorylation through the inhibition of protein kinase β/Akt in human endothelial cells. *Mol Cell Biol* 2002; **22:** 8467–8477.
16. Kato M, Blanton R, Wang GR, Judson TJ, Abe Y, Myoishi M, et al. Direct binding and regulation of Rho a protein by cyclic GMP-dependent protein kinase Iα. *J Biol Chem* 2012; **287:** 41342–41351.
17. Pelouch V, Dixon IM, Golfman L, Beamish RE, Dhalla NS. Role of extracellular matrix proteins in heart function. *Mol Cell Biochem* 1993; **129:** 101–120.
18. Nong Z, O'Neil C, Lei M, Gros R, Watson A, Rizkalla A, et al. Type I collagen cleavage is essential for effective fibrotic repair after myocardial infarction. *Am J Pathol* 2011; **179:** 2189–2198.
19. Oka T, Hikoso S, Yamaguchi O, Taneike M, Takeda T, Tamai T, et al. Mitochondrial DNA that escapes from autophagy causes inflammation and heart failure. *Nature* 2012; **485:** 251–255.
20. Shiojima I, Sato K, Izumiya Y, Schiekofer S, Ito M, Liao R, et al. Disruption of coordinated cardiac hypertrophy and angiogenesis contributes to the transition to heart failure. *J Clin Invest* 2005; **115:** 2108–2118.
21. Nakajima S, Ohashi J, Sawada A, Noda K, Fukumoto Y, Shimokawa H. Essential role of bone marrow for microvascular endothelial and metabolic functions in mice. *Circ Res* 2012; **111:** 87–96.
22. Fukumoto Y, Deguchi JO, Libby P, Rabkin-Aikawa E, Sakata Y, Chin MT, et al. Genetically determined resistance to collagenase action augments interstitial collagen accumulation in atherosclerotic plaques. *Circulation* 2004; **110:** 1953–1959.
23. Liu X, Wu H, Byrne M, Jeffrey J, Krane S, Jaenisch R. A targeted mutation at the known collagenase cleavage site in mouse type I collagen impairs tissue remodeling. *J Cell Biol* 1995; **130:** 227–237.
24. Zhao W, Byrne MH, Boyce BF, Krane SM. Bone resorption induced by parathyroid hormone is strikingly diminished in collagenase-resistant mutant mice. *J Clin Invest* 1999; **103:** 517–524.
25. Zhao W, Byrne MH, Wang Y, Krane SM. Osteocyte and osteoblast apoptosis and excessive bone deposition accompany failure of collagenase cleavage of collagen. *J Clin Invest* 2000; **106:** 941–949.
26. Abe K, Tawara S, Oi K, Hizume T, Uwatoku T, Fukumoto Y, et al. Long-term inhibition of rho-kinase ameliorates hypoxia-induced pulmonary hypertension in mice. *J Cardiovasc Pharmacol* 2006; **48:** 280–285.
27. Wang W, Kagaya Y, Asaumi Y, Fukui S, Takeda M, Shimokawa H. Protective effects of recombinant human erythropoietin against pressure overload-induced left ventricular remodeling and premature death in mice. *Tohoku J Exp Med* 2011; **225:** 131–143.
28. Fukui S, Fukumoto Y, Suzuki J, Saji K, Nawata J, Shinozaki T, et al. Diabetes mellitus accelerates left ventricular diastolic dysfunction through activation of the renin-angiotensin system in hypertensive rats. *Hypertension Res* 2009; **32:** 472–480.
29. Satoh K, Nigro P, Zeidan A, Soe NN, Jaffre F, Oikawa M, et al. Cyclophilin A promotes cardiac hypertrophy in apolipoprotein E-deficient mice. *Arterioscler Thromb Vasc Biol* 2011; **31:** 1116–1123.
30. Dai DF, Johnson SC, Villarin JJ, Chin MT, Nieves-Cintron M, Chen T, et al. Mitochondrial oxidative stress mediates angiotensin II-induced cardiac hypertrophy and Gαq overexpression-induced heart failure. *Circ Res* 2011; **108:** 837–846.
31. Ghofrani HA, Olschewski H, Seeger W, Grimminger F. Sildenafil

for treatment of severe pulmonary hypertension and commencing right-heart failure. *Pneumologie* 2002; **56:** 665–672.
32. Voelkel NF, Gomez-Arroyo J, Abbate A, Bogaard HJ, Nicolls MR. Pathobiology of pulmonary arterial hypertension and right ventricular failure. *Eur Resp J* 2012; **40:** 1555–1565.
33. Giaid A, Saleh D. Reduced expression of endothelial nitric oxide synthase in the lungs of patients with pulmonary hypertension. *New Engl J Med* 1995; **333:** 214–221.
34. Do.e Z, Fukumoto Y, Takaki A, Tawara S, Ohashi J, Nakano M, et al. Evidence for Rho-kinase activation in patients with pulmonary arterial hypertension. *Circ J* 2009; **73:** 1731–1739.
35. Laviades C, Varo N, Fernandez J, Mayor G, Gil MJ, Monreal I, et al. Abnormalities of the extracellular degradation of collagen type I in essential hypertension. *Circulation* 1998; **98:** 535–540.
36. Yasmin, McEniery CM, Wallace S, Dakham Z, Pulsalkar P, Maki-Petaja K, et al. Matrix metalloproteinase-9 (MMP-9), MMP-2, and serum elastase activity are associated with systolic hypertension and arterial stiffness. *Arterioscler Thromb Vasc Biol* 2005; **25:** 372–378.
37. Izumiya Y, Shiojima I, Sato K, Sawyer DB, Colucci WS, Walsh K. Vascular endothelial growth factor blockade promotes the transition from compensatory cardiac hypertrophy to failure in response to pressure overload. *Hypertension* 2006; **47:** 887–893.
38. Sano M, Minamino T, Toko H, Miyauchi H, Orimo M, Qin Y, et al. P53-induced inhibition of HIF-1 causes cardiac dysfunction during pressure overload. *Nature* 2007; **446:** 444–448.
39. Bogaard HJ, Natarajan R, Henderson SC, Long CS, Kraskauskas D, Smithson L, et al. Chronic pulmonary artery pressure elevation is insufficient to explain right heart failure. *Circulation* 2009; **120:** 1951–1960.
40. Umar S, van der Valk EJ, Schalij MJ, van der Wall EE, Atsma DE, van der Laarse A. Integrin stimulation-induced hypertrophy in neonatal rat cardiomyocytes is NO-dependent. *Mol Cell Biochem* 2009; **320:** 75–84.
41. Partovian C, Adnot S, Eddahibi S, Teiger E, Levame M, Dreyfus P, et al. Heart and lung VEGF mRNA expression in rats with monocrotaline- or hypoxia-induced pulmonary hypertension. *Am J Physiol* 1998; **275:** H1948–H1956.
42. Ichinose F, Bloch KD, Wu JC, Hataishi R, Aretz HT, Picard MH, et al. Pressure overload-induced LV hypertrophy and dysfunction in mice are exacerbated by congenital NOS3 deficiency. *Am J Physiol* 2004; **286:** H1070–H1075.
43. William GS. Matrix metalloproteinases in angiogenesis: A moving target for therapeutic intervention. *J Clin Invest* 1999; **103:** 1237–1241.
44. Satoh K, Fukumoto Y, Shimokawa H. Rho-kinase: Important new therapeutic target in cardiovascular diseases. *Am J Physiol* 2011; **301:** H287–H296.
45. Ikeda S, Fukumoto Y, Shimizu T, Shimokawa H. Cardiac-specific overexpression of dominant-negative Rho-kinase suppresses pressure overload-induced right and left heart failure in mice. *Circ J* 2013; **77**(Suppl I)**:** I-2905.
46. Rikitake Y, Liao JK. Rho GTPases, statins, and nitric oxide. *Circ Res* 2005; **97:** 1232–1235.
47. Shimokawa H, Rashid M. Development of Rho-kinase inhibitors for cardiovascular medicine. *Trends Pharmacol Sci* 2007; **28:** 296–302.
48. Qipshidze N, Tyagi N, Metreveli N, Lominadze D, Tyagi SC. Autophagy mechanism of right ventricular remodeling in murine model of pulmonary artery constriction. *Am J Physiol* 2012; **302:** H688–H696.
49. Dorfmuller P, Perros F, Balabanian K, Humbert M. Inflammation in pulmonary arterial hypertension. *Eur Resp J* 2003; **22:** 358–363.
50. Maron BA, Michel T. Subcellular localization of oxidants and redox modulation of endothelial nitric oxide synthase. *Circ J* 2012; **76:** 2497–2512.
51. Imanaka-Yoshida K. Tenascin-C in cardiovascular tissue remodeling: From development to inflammation and repair. *Circ J* 2012; **76:** 2513–2520.
52. Abe K, Toba M, Alzoubi A, Ito M, Fagan KA, Cool CD, et al. Formation of plexiform lesions in experimental severe pulmonary arterial hypertension. *Circulation* 2010; **121:** 2747–2754.

Supplementary Files

Supplementary File 1

Methods

Figure S1. Hypoxia-induced angiogenesis is impaired in eNOS$^{-/-}$ mice.

Figure S2. Hypoxia-induced angiogenesis is not impaired in Col$^{R/R}$ mice.

Figure S3. Hypoxia-induced rho-kinase activity is enhanced in eNOS$^{-/-}$ mice.

Figure S4. Hypoxia-induced rho-kinase activity is enhanced in Col$^{R/R}$ mice.

Figure S5. Enhanced autophagy in eNOS$^{-/-}$ and Col$^{R/R}$ mice.

Table S1. Characteristics of controls and PH patients with RV failure

Table S2. Anatomical data of WT and eNOS$^{-/-}$ mice after 3-week hypoxia

Table S3. Anatomical data for WT and Col$^{R/R}$ mice after 3-week hypoxia

Please find supplementary file(s);
http://dx.doi.org/10.1253/circj.CJ-13-1586